Qeios

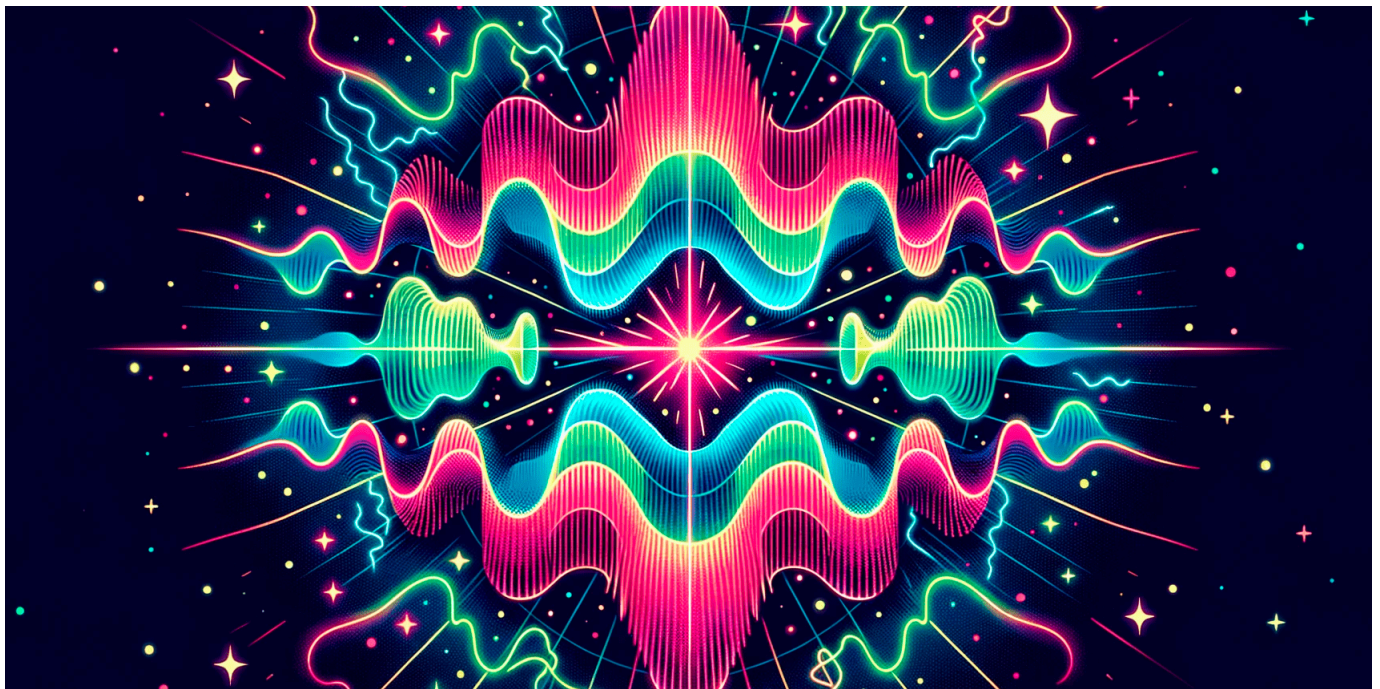# Numerical Evaluation of a Soliton Pair with Long Range Interaction

Joachim Wabnig, Josef Resch, Dominik Theuerkauf, Fabian Anmasser, Manfried Faber

Numerical Evaluation of a Soliton Pair with Long Range Interaction

**Joachim Wabnig, Josef Resch, Dominik Theuerkauf,
Fabian Anmasser and Manfried Faber**

Technische Universität Wien, Atominstitut, Stadionalee 2, 1020 Wien, Austria

Abstract

We determine the interaction energy of electric or magnetic monopole pairs, sources and sinks of a Coulombic field. The monopoles are represented by topological solitons of finite size and mass, described by a field of SO(3) rotations without any divergences. Such monopoles feel at large distances a pure Coulombic interaction. A crucial test for the physical interpretation of these monopoles is a classical running of the charge at small distances, expected from the finite soliton size. We investigate in detail a first observation of the increase of the effective charge at a few soliton radii in this purely Coulombic system and compare it with the running of the coupling in perturbative QED.

1 Introduction

In Refs. [1, 2] we proposed a dynamical model with only three degrees of freedom (dofs) for the dynamics of monopoles, the model of topological particles (MTP). This model does not suffer from any singularities as Dirac monopoles and other field models do. Particles are identified by topological quantum numbers. One of them is the charge, topologically quantised in units of an elementary charge. Depending on the interpretation, charges can be either electric or magnetic. They show Coulombic behaviour. Masses of particles originate in field energy and opposite charges can annihilate. The model and its many predictions were extensively discussed in Ref. [2].

Magnetic monopoles were invented by Dirac in 1931 [3, 4] as quantised singularities in the electromagnetic field. He found that their existence would explain the quantisation of electric charge, proven in Millikan's experiments [5] but not explained by Maxwell theory [6]. Dirac monopoles have two types of singularities, the Dirac string, a line-like singularity connecting monopoles and antimonopoles, and the singularity in the centre of the monopole, a singularity analogous to the singularity of point-like electrons. Wu and Yang succeeded to formulate magnetic monopoles without the line-like singularities of the Dirac strings by using either a fibre-bundle construction with two different gauge fields [7], one for the northern and one for the southern hemisphere of the monopole, or by a non-abelian SU(2) gauge field in 3+1D [8, 9]. The non-abelian Wu-Yang monopoles still suffer from the point-like singularities in the centre. There are monopole solutions without any singularity in the Georgi-Glashow model [10], the 'tHooft-Polyakov monopoles [11, 12]. The Georgi-Glashow model, formulated in 3+1D, has 15 dofs, an adjoint Higgs field with three dofs and an SU(2) gauge field with $4 \cdot 3 = 12$ field components. Only one dof is needed for the Sine-Gordon model [13], a model in 1+1D. It is most interesting that in addition to waves, it has kink and anti-kink solutions which interact with each other. The kink-antikink configurations are attracting and the kink-kink configurations repelling. The simplicity of the Sine-Gordon model inspired Skyrme [14, 15, 16, 17, 18] to a model in 3+1D with a scalar SU(2)-valued field, i.e. three dofs. Stable topological solitons (Skyrmions) emerge in that model with the properties of particles, interacting at short range. MTP was also inspired by the simplicity and physical content of the Sine-Gordon model, it was first formulated in [1]. It uses the SO(3) dofs of a spatial Dreibeins (triads). Since these can be mapped to SU(2), the double covering group of SO(3), it has some relation to the Skyrme model and shares its philosophy. Whereas Skyrme formulated his model for the strong interaction, MTP describes different physics, the electromagnetic interaction. In

the Skyrme model the unit matrix represents the unique vacuum, whereas the MTP vacuum has a twofold degeneracy on the equatorial sphere S^2_{equ} of S^3 in order to describe the long range, Coulombic interaction. The relations of MTP to electrodynamics and symmetry breaking were discussed in [2, 19, 20, 21].

In this article, we want to concentrate on numerical determinations of the interaction energy for a pair of charges, represented by soliton-antisoliton pairs and especially on the tiny deviations from pure Coulombic behaviour. Due to the non-existence of magnetic monopoles, comparisons to nature – the main duty of physics – are possible only for electric charges and the predictions of QED.

In Sect. 2 we repeat the formulation and some basic properties of the model, in Sect. 3 we show first results of the calculations and compare the results to perturbative QED. We find astonishing analogies of the short distance behaviour of the interaction. In the appendix A we present the numerical formulation in cylindrical coordinates and show some informative diagrams.

2   Summary of MTP

As expounded in Ref. [2] we use the SO(3) degrees of freedom (dofs) of spatial Dreibeins to describe electromagnetic phenomena. The calculations get simpler using SU(2) matrices,

$$Q(x) = \mathrm{e}^{-\mathrm{i}\alpha(x)\vec{\sigma}\vec{n}(x)} = \underbrace{\cos\alpha(x)}_{q_0(x)} - \mathrm{i}\vec{\sigma}\,\underbrace{\vec{n}\sin\alpha(x)}_{\vec{q}(x)} \in SU(2) \cong \mathbb{S}^3 \tag{2.1}$$

in Minkowski space-time as field variables, where arrows indicate vectors in the 3D algebra of su(2) with the basis vectors represented by the Pauli matrices σ_i. The Lagrangian of MTP reads,

$$\mathcal{L}_{\text{MTP}}(x) := -\frac{\alpha_f \hbar c}{4\pi} \left(\frac{1}{4}\, \vec{R}_{\mu\nu}(x)\vec{R}^{\mu\nu}(x) + \Lambda(x) \right) \quad \text{with} \quad \Lambda(x) := \frac{q_0^6(x)}{r_0^4}, \tag{2.2}$$

with

$$\vec{R}_{\mu\nu} := \vec{\Gamma}_\mu \times \vec{\Gamma}_\nu \quad \text{and} \quad (\partial_\mu Q)\, Q^\dagger =: -\mathrm{i}\vec{\sigma}\vec{\Gamma}_\mu. \tag{2.3}$$

We get contact with nature by relating the electromagnetic field strength tensor to the dual of the curvature tensor $\vec{R}_{\mu\nu}$,

$$\vec{F}_{\mu\nu} := -\frac{e_0}{4\pi\epsilon_0}\,{}^\star\!\vec{R}_{\mu\nu}. \tag{2.4}$$

At large distances d from the sources, measured in units of the soliton scale parameter r_0, the non-abelian field strength gets abelian,

$$\vec{F}_{\mu\nu} \overset{d \gg r_0}{\to} (\vec{F}_{\mu\nu}\vec{n})\vec{n}. \tag{2.5}$$

MTP has four different classes of topologically stable single soliton configurations. Their representatives read,

$$n_i(x) = \pm\frac{x^i}{r}, \quad \alpha(x) = \frac{\pi}{2} \mp \arctan\frac{r_0}{r} = \begin{cases} \arctan\frac{r}{r_0} \\ \pi - \arctan\frac{r}{r_0} \end{cases} \tag{2.6}$$

The imaginary part of their Q-fields are schematically depicted in Table 1. The fields (2.6) are solutions of the non-linear Euler-Lagrange equations [2]. They differ in two quantum numbers related to charge and spin. In the minimum of the potential the Q-field (2.1) is purely imaginary. Therefore, the sign Z of the $\vec{n}$-field in Eq. (2.6) decides about the charge quantum number defined by a map $\Pi_2(\mathbb{S}^2_{\text{equ}})$ with $\mathbb{S}^2_{\text{equ}}$ the equatorial sphere of $\mathbb{S}^3$. A monopole is regular, but looks at large distances like a hedgehog singularity, unit vectors pointing in all radial directions. Such singularities can be removed by annihilation only. This explains Gauß's law, the conservation of electric/magnetic flux through closed surfaces around the singularities, mapped to the $\mathbb{S}^2_{\text{equ}}$ target space.

Field configurations are further characterised by the number $\mathcal{Q}$ of coverings of $\mathbb{S}^3$, by the map $\Pi_3(\mathbb{S}^3)$. With the sign of $\mathcal{Q}$ we define an internal chirality χ and with the absolute value of $\mathcal{Q}$ the spin quantum number s,

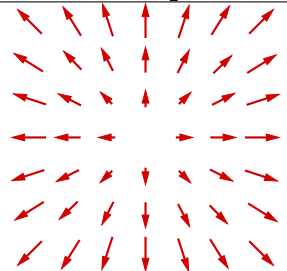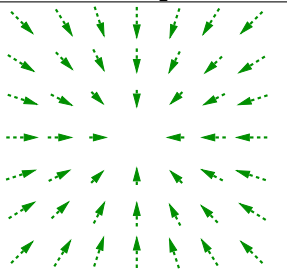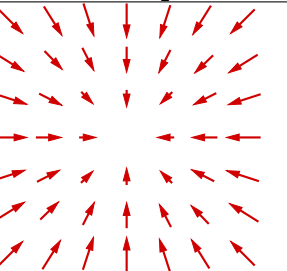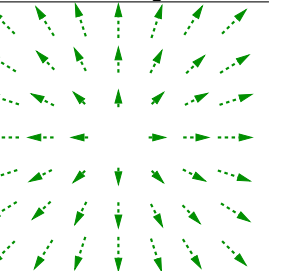$$\mathcal{Q} = \chi \cdot s \quad \text{with} \quad s := |\mathcal{Q}|. \tag{2.7}$$

$\vec{n} = \vec{r}/r$	$\vec{n} = -\vec{r}/r$	$-\vec{n} = \vec{r}/r$	$\vec{n} = \vec{r}/r$
$q_0 \geq 0$	$q_0 \leq 0$	$q_0 \geq 0$	$q_0 \leq 0$
$Z = 1$	$Z = -1$	$Z = -1$	$Z = 1$
$\mathcal{Q} = \frac{1}{2}$	$\mathcal{Q} = \frac{1}{2}$	$\mathcal{Q} = -\frac{1}{2}$	$\mathcal{Q} = -\frac{1}{2}$

Table 1: Scheme of single soliton configurations. The fields $\vec{n}$ and q_0 and the topological quantum numbers Z and $\mathcal{Q}$ are indicated. The diagrams show the imaginary components $\vec{q} = \vec{n}\sin\alpha$ of the soliton field, in full red for the hemisphere with $q_0 > 0$ and in dashed green for $q_0 < 0$.

The spin quantum number of two-soliton configurations indicates that χ can be related to the sign of the magnetic spin quantum number.

The configurations within each of the four classes may differ by Poincaré transformations. The rest mass of solitons,

$$E_0 = \frac{\alpha_f \hbar c}{r_0}\frac{\pi}{4},\tag{2.8}$$

can be adjusted to the electron rest energy $m_e c_0^2 = 0.510\,998\,95$ MeV by choosing,

$$r_0 = 2.213\,205\,16\ \text{fm},\tag{2.9}$$

a scale which is of the order of the classical electron radius. The four parameters r_0, c_0, E_0 and e_0 correspond to the natural scales of the four quantities length, time, mass and charge of the SI, of the Système international d'unités, involved in this model. Eq. (2.8) can therefore be interpreted as a relation between α_f and $\hbar$.

3 The Coulomb potential and its numerical determination

Two solitons of different charge can be combined to two topological different field configurations. Schematic diagrams for such configurations are shown in Fig. 1. An example of its modifications by the minimisation procedure is shown in the appendix in Fig. 8.

From the analytical calculations in Ref. [19] we know that MTP respects the inhomogeneous Maxwell equations. Therefore, we expect for point-like charges the classical Coulombic behaviour at large distances d between the charges of the dipole. This reads after adjusting the asymptotic energies

$$E_{\text{cl}}(d) = E_\infty - \frac{\alpha_f \hbar c_0}{d}\quad\text{with}\quad \alpha_f = 137.036, \hbar c_0 = 197.327\,\text{MeV fm}.\tag{3.1}$$

In Fig. 2 we compare $E_{\text{cl}}(d)$ to the numerical results for the energy $E(d)$, see Eq. (A.9), of the dipole in the spin singlet state. The left diagram depicts the comparison in the region $24\,a \leq \bar{d} \leq 420\,a$ in steps $\Delta\bar{d} = 2\,a$ for $a = r_0/3 = 0.7377\,\text{fm}$. At large distances d compared to the soliton radius parameter r_0, the size of Coulomb attraction can be determined relative easily. But deviations from the Coulombic behaviour, as shown in the right diagram of Fig. 2, are tiny and need high precision calculations. There are no data for distances smaller than $d = 24\,a$, since the soliton pair cannot be stabilised just by fixing the soliton field to $Q = 1$ at the positions of soliton centers.

We describe these small deviations by a d-dependence of the fine structure constant

$$E(d) = E_\infty - \frac{\alpha(d)\,\hbar c_0}{d}.\tag{3.2}$$

In Fig. 3 we can nicely observe whether the asymptotic energy E_∞ is well chosen, as tiny variations of E_∞ destroy the asymptotic behaviour of $\alpha(d)$ at large d. The running of the coupling $\alpha(d)$ already detected in Fig. 2 is clearly seen in Fig. 3 below distances of $50\,\text{fm}$.
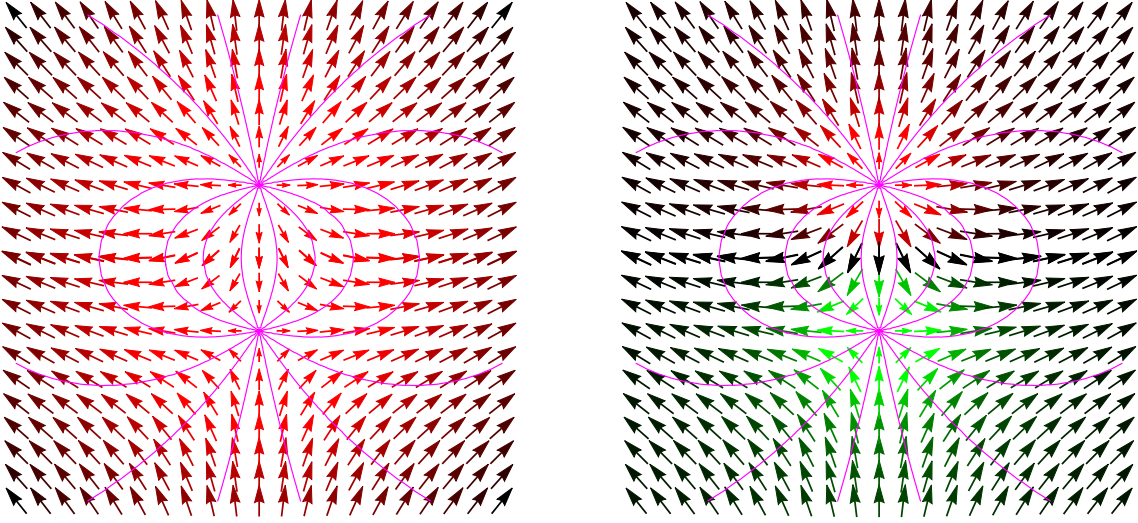
Figure 1: Schematic diagrams depicting the imaginary part $\vec{q} = \vec{n}\sin\alpha$ of the Q-field of two opposite unit charges by arrows. The lines represent some electric flux lines. We observe that they coincide with the lines of constant $\vec{n}$-field. The configurations are rotational symmetric around the axis through the two charge centres. In the red/green arrows, we encrypt also the positive/negative values of $q_0 = \cos\alpha$. For $q_0 \to 0$ the arrows are getting darker or black. The left configuration belongs to the topological quantum numbers $\mathcal{Q} = S = 0$ and the right one to $\mathcal{Q} = S = 1$, where S is the total spin quantum number of the configuration. The numerical calculations will be presented for the spin singlet case.
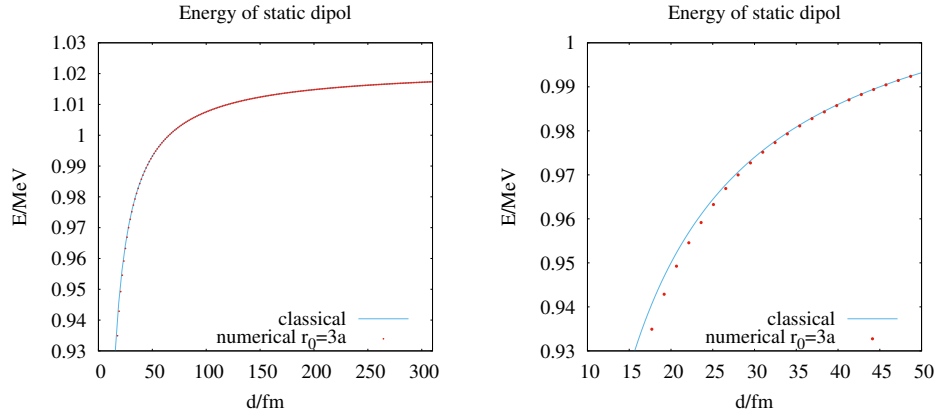

Figure 2: Comparison between the classical Coulomb potential $E_{\mathrm{cl}}(d)$ and the numerical values of the energy $E(d)$ according to Eq. (A.9) of a static electron-positron pair as a function of the separation d between the two charges. Due to the finite size of solitons we observe deviations of the energy of the static dipole (red circles) from the classical value for point-like sources (full blue line).

To be able to reach smaller values of d before the attraction gets too strong and the dipole is collapsing, Ref. [22] suggested to minimise the energy functional $E_{\min}$ of Eq. (A.10) which suppresses photonic excitations. In the computations, see Fig. 4, it turns out that it helps to approach shorter distances, but at distances of around 30 fm it may lead to nonphysical stiffness of the fields and to a strong reduction of $\alpha(d)$. This nonphysical behaviour starts to be observable around $\lambda = 0.005/a^2$. Looking carefully at Fig. 3 we see a similar but very tiny additional stiffness also in the $\lambda = 0$ results. It is not yet clear whether the minimum in $\alpha(d)/\alpha_f$ at $d \approx 50\tilde{\mathrm{fm}}$ is a physical effect or an error of the approximation, e.g. of the boundary conditions. Due to its small size this effect is not really visible in Fig. 4 at $\lambda = 0$.
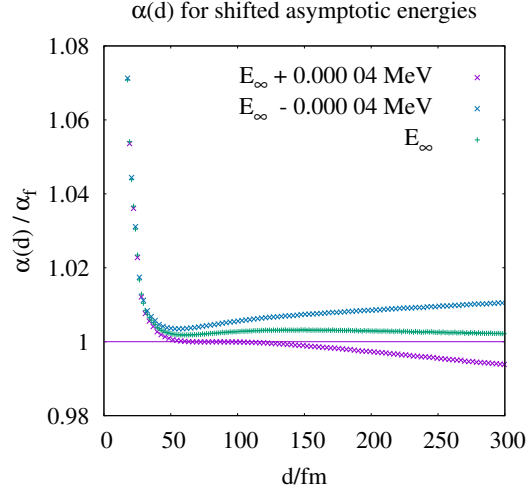
Figure 3: Influence of the choice of E_∞ to the asymptotic behaviour of $\alpha(d)$ according to Eq. (3.2). Observe that tiny variations of E_∞ lead to wrong asymptotic behaviour at large charge separations.
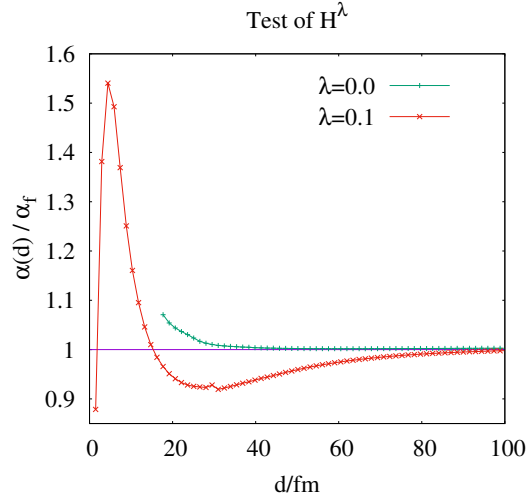

Figure 4: The suppression of photonic excitations by the λ-dependent term in Eq. (A.10) allows to approach shorter distances but leads to an nonphysical reduction of $\alpha(d)$ around distances of 30 fm, as can be clearly observed for $\lambda = 0.1/a^2$.

For tiny $\lambda \leq 0.005/a^2$ we can proceed to smaller distances d. The corresponding data is plotted in Fig. 5. With the above described careful and effortful determination of the interaction potential we observe nice Coulombic behaviour with constant coupling strength at distances above 50 fm and a sharp increase of the effective charge at distances below 40 fm. This is the first observation of a running of the charge at the classical level in a pure Coulombic system.

The only physical effect, reasonable to compare with, is the rise of the coupling in perturbative QED as described in Ref. [23]. For comparison we show the prediction of first order perturbation theory and its long distance approximation which is well known as Uehling potential.

In QED the interaction between charges is described by photon exchange. The algebraic form of the photon propagator determines therefore the strength of the interaction. The perturbative corrections to the tree level photon propagator are divergent. Already the first order contribution, shown by the electron-loop diagram in Fig. 6, is divergent and needs regularisation and renormalisation. A perfect regularisation method is dimensional regularisation. Its success is understood from the conservation of symmetries besides scale invariance. In the renormalisation procedure an infinite photon self-energy is subtracted. It is adjusted in such a way that the divergence of the photon propagator is cancelled. Invariance under the finite terms which are subtracted in this
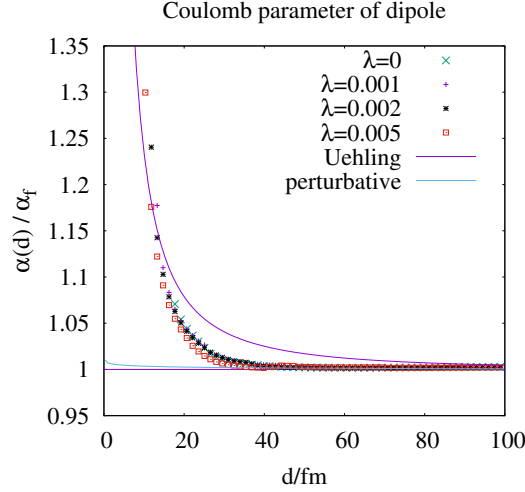
Figure 5: The rise of $\alpha(d)$ at short separation d of the monopole pair is clearly seen in the data points for various λ values. These numerical results are compared to the analytical formulae of first order perturbation theory (3.3) in QED and its long distance approximation (3.4). The strong attraction at short distances does not allow to stabilise the distance d of the charges just by fixing the centers of solitons with the energy functional (A.9). One can get to shorter distances using the functional of Eq. (A.10) for the minimisation procedure. For tiny values of λ the potential is only weakly distorted.
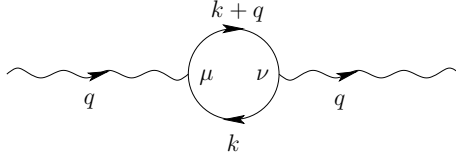

Figure 6: Electron-loop diagram as contribution to the photon propagator at four-momentum q in first order perturbation theory.

procedure requests a modification of the electric charge at large momentum transfers and small distances. This is usually interpreted as a modification of the photon structure by virtual electron-positron pairs. This prediction of perturbation theory leads to a radial dependent fine structure constant

$$\alpha(r) = \alpha_f \Big\{ 1 + \underbrace{\frac{2\alpha_f}{3\pi} \int_1^\infty \mathrm{d}\gamma \frac{\mathrm{e}^{-2\mu\gamma r}}{\gamma} \sqrt{1 - \frac{1}{\gamma^2}} \Big(1 + \frac{1}{2\gamma^2} \Big)}_{\Delta(r)} \Big\}, \tag{3.3}$$

where μ is the reduced Compton wavelength of electrons and γ is the relativistic γ factor for the mass of a moving particle. The correction can be evaluated by numerical integration and leads to the curve "perturbative" in Fig. 5. The approximation for large μr reads [23]

$$\alpha(r) = \alpha_f \Big\{ 1 + \frac{\alpha_f}{\sqrt{2\pi}} \frac{\mathrm{e}^{-2\mu r}}{(2\mu r)^{3/2}} \Big\}. \tag{3.4}$$

It is depicted for comparison in Fig. 5 as approximation to the "Uehling" potential. This large distance approximation reflects the numerical results of the running of the charge at the expected order of magnitude.

4 Conclusion

In the model of topological particles we can describe electric or magnetic monopoles and their interaction without any divergencies. If the finite masses of the stable soliton states are compared with the electron mass, the finite size r_0 of the solitons is of the order of the classical electron

6

radius. Since analytic solutions of this model are known for one-particle systems only, we have to analyse the interacting systems of two monopoles numerically with high precision. In this first calculation we investigate the classical monopole-antimonopole potential in the spin zero state. At large separation d of the dipole the potential has purely $1/d$ behaviour. We observe for the first time the running of the charge at a classical level in a pure Coulombic system. It is a natural question how this running compares to the running of the coupling in QED. We would like to underline as important outcome of the computations that the increase of the coupling appears at the same length scale as predicted by the long distance approximation of perturbative QED, see Fig. 5.

In further calculations the accuracy of the calculation should be enlarged using adaptive lattices. This would allow to diminish the influence of boundary effects. Since these first numerical calculations are done in the static limit one should expect major modifications for more realistic dynamical scenarios. Especially interesting would be to insert the potential which results from such more detailed calculation in the Schrödinger and Dirac equation [24]. This would result in shifts of the Dirac energy levels which could be compared with the Lamb shift. Further calculations should be done in the spin one state and for the repulsive system of two equal charges where the cylindrical symmetry is lost.

A   Dipoles on a cylindrical lattice

According to the Lagrangian (2.2) there are two contributions to the energy density of a static dipole,

$$\mathcal{H} \stackrel{(2.2)}{=} \frac{\alpha_f \hbar c}{4\pi} \left(\frac{1}{4} \vec{R}_{ij} \vec{R}^{ij} + \Lambda \right) =: \mathcal{H}_{\text{cur}} + \mathcal{H}_{\text{pot}}, \tag{A.1}$$

the electric part of the curvature energy and the potential energy. A detailed derivation of these energy contributions of the $Q(x)$ field in cylindrical coordinates was given in [22]. The curvature energy reads in these coordinates,

$$\mathcal{H}_{\text{cur}} = \frac{\epsilon_0}{2} \left(\vec{E}_r^2 + \vec{E}_\varphi^2 + \vec{E}_z^2 \right) = \frac{\alpha_f \hbar c}{8\pi} \frac{1}{r^2} \left\{ q_r^2 \left[(\partial_z q_0)^2 + (\partial_z q_r)^2 + (\partial_z q_z)^2 \right] \right.$$
$$\left. + \frac{r^2}{q_0^2} \left(\partial_r q_r \partial_z q_z - \partial_z q_r \partial_r q_z \right)^2 + q_r^2 \left[(\partial_r q_0)^2 + (\partial_r q_r)^2 + (\partial_r q_z)^2 \right] \right\}. \tag{A.2}$$

Due to the cylindrical symmetry of the field configurations in Fig. 1 it is sufficient to restrict the numerical integrations to a lattice in the rz-plane, see Fig. 7. Inside the lattice, we minimise the
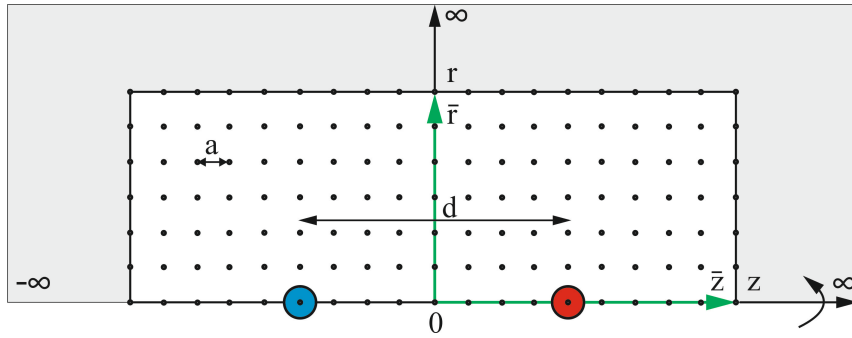

Figure 7: Two solitons of opposite charge are separated by a distance d on a discrete lattice in the rz plane. The total number of points is $n_r \times 2n_z$ and the lattice constant in both directions is a.

energy according to the numerical formulation of the MTP Lagragian. Outside, we use Maxwell's electrodynamics [6] to calculate the energy. The numerical computations of dipole field configurations were built up on the algorithms discussed in [25, 26, 27] and their accuracy was tested in [22] by applying it to the analytical solvable monopole configuration. The coordinates in radial- and z direction are denoted by $\bar{r} \in \{0, 1, \ldots, n_r\}$ and $\bar{z} \in \{-n_z, -n_z + 1, \ldots, n_z\}$, respectively. The radius of a soliton, $\bar{r}_0 \in \mathbb{N}$, determines the length-scale and thereby the lattice spacing,

$$a \stackrel{(2.9)}{=} \frac{2.21\text{fm}}{\bar{r}_0}. \tag{A.3}$$

A numerical gradient minimisation algorithm is used to find the dipole configurations, which minimises the total energy according to Eq. (A.1) for given distance $d = a\bar{d}$ between the opposite charges.

A good guess for the initial configuration helps to reduce the run-time of the computation. For the real part of the initial Q-field we get from the profile function of a single monopole,

$$q_0(r, z > 0) = \frac{\bar{r}_0}{\sqrt{\bar{r}_0^2 + \bar{r}^2 + (\bar{z} - \frac{\bar{d}}{2})^2}}, \qquad q_0(r, z \leq 0) = \frac{\bar{r}_0}{\sqrt{\bar{r}_0^2 + \bar{r}^2 + (\bar{z} + \frac{\bar{d}}{2})^2}}. \qquad (A.4)$$

The modulus of the vector part of the Q-field reads,

$$|\vec{q}(x)| \overset{(2.1)}{=} \sqrt{1 - q_0(x)^2}. \qquad (A.5)$$

An appropriate initial direction $\vec{n}$ of the $\vec{q}$ field we get from the coincidence between electric field lines and lines of constant $\vec{n}$-field which we observe in Fig. 1. The field lines are defined by the differential equation,

$$\frac{\mathrm{d}r}{E_r} = \frac{\mathrm{d}z}{E_z}, \qquad (A.6)$$

with

$$E_r(r, z) = \frac{e_0}{4\pi\epsilon_0} \left(\frac{r}{(r^2 + (z + \frac{d}{2})^2)^{3/2}} - \frac{r}{(r^2 + (z - \frac{d}{2})^2)^{3/2}} \right),$$
$$E_z(r,) = \frac{e_0}{4\pi\epsilon_0} \left(\frac{z + \frac{d}{2}}{(r^2 + (z + \frac{d}{2})^2)^{3/2}} - \frac{z - \frac{d}{2}}{(r^2 + (z - \frac{d}{2})^2)^{3/2}} \right). \qquad (A.7)$$

After solving the differential Eq. (A.6), we find an analytical expression for the initial polar angle of the $\vec{q}$ field,

$$\theta(r, z) = \arccos \left(1 + \frac{z - \frac{d}{2}}{\sqrt{r^2 + (z - \frac{d}{2})^2}} - \frac{z + \frac{d}{2}}{\sqrt{r^2 + (z + \frac{d}{2})^2}} \right). \qquad (A.8)$$

Up to now, only points on the lattice are included in the energy calculation. Outside the lattice, we use Maxwell's electrodynamics to take the curvature energy into account. The error, for neglecting potential and tangential energy components outside the lattice, was shown to be tiny ($< 0.2\%$) for a single monopole, if the distance from the soliton core to the lattice boundaries is greater than $10a$ [22]. Hence, we find the energy outside the lattice by $H_{\mathrm{out}} = \frac{\epsilon_0}{2} \int_{\mathbb{R}^3 \setminus \mathrm{latt}} \mathrm{d}^3 x |\vec{E}|^2$, which is numerically integrated using a trapezoidal summation, with the electric field strength given by Eq. A.7.

The principle of energy minimisation is exploited to find the dipole field configuration and its associated energy. The minimisation algorithm is taken from https://de.mathworks.com/matlabcentral/fileexchange/75546-conjugate-gradient-minimisation. It is a more dimensional conjugate gradient method to find a local minimum of an energy functional depending on the Q field components at each lattice point, $E = E(q_0^i, q_r^i, q_z^i)$ with $i \in [1, 2, ..., n_r(2n_z + 1)]$,

$$E = \int_{\mathrm{lattice}} \mathrm{d}^3 x \; \mathcal{H}_{\mathrm{lat}} + H_{\mathrm{out}}, \qquad (A.9)$$

where $\mathcal{H}_{\mathrm{lat}}$ is the lattice version of $\mathcal{H}$ of Eq. (A.1).

Fixing the centre of solitons only, however, for small dipole distances d annihilation of the two solitons is observed. To suppress this behaviour, it was suggested in Ref. [22] to smooth the soliton field by adding to the energy functional a term,

$$E_{\mathrm{min}} := E + \lambda \frac{\alpha_f \hbar c}{a} \sum_i \left(\frac{\partial}{\partial \bar{x}_i} \frac{\vec{q}}{|\vec{q}|} \right)^2, \quad i = \{\bar{r}, \bar{z}\}. \qquad (A.10)$$

in the minimisation process, where $\lambda = \bar{\lambda}/a^2$. During the computations, it became clear that this additional term tends to suppress the interaction between the solitons. Therefore, we could apply tiny values of $\bar{\lambda}$ only. This was sufficient to approach smaller distances.

The parameters, used for the minimisation process are listed in table 2.

Parameter	Description	Used value
i_{max}	Max. number of iterations	5000
Δ_{grad}	Min. gradient difference for two consecutive iterations	1e-6
Δ_{fun}	Min. energy difference for two consecutive iterations	1e-30
Δ_{com}	Lower bound on the step size of the norm of the Q field	1e-30

Table 2: Input parameters for the energy minimisation algorithm.

The lattice spacing we fix to $a \stackrel{(A.3)}{=} r_0/3 = 0.738$ fm. This spacing is small enough to get a reasonable approximation to the rest energy of electrons.

For a dipole, it is not possible to use periodic boundary conditions. While minimising the energy, we fix the soliton field Q at the edge of the lattice $\bar{r} = 0, \bar{r} = n_r, \bar{z} = \pm n_z$ according to the initial configuration discussed in Sect. A. This implies the assumption $q_0 = 0$ outside the lattice, and leads to a small error in the potential energy which is difficult to avoid.

Nevertheless, boundary conditions have large influence on the numerical results. For fixed lattice sizes $n_r \times (2n_z + 1)$ and varying size d of the dipole, we are unable to reach large d values due to boundary effects. It turns out to be much better to increase the lattice size with increasing d keeping the distance from the boundary constant. The lattice sizes we are using for our calculations are in r- and z-directions by 45 lattice spacings larger than the relative distance d between the charges. We use $n_r = 45$ and $n_z = \frac{\bar{d}}{2} + 45$ and all even distances $\bar{d} \leq 420$.

Due to the finite size of the lattice there remains a deviation of the asymptotic energy E_∞ of the dipole from the mass of two non-interacting solitons, $2m_e c_0^2 = 1.021\,997\,90$ MeV. Since we fix the centers of solitons at lattice sites, we get a weak even-odd effect on lattice sizes for E_∞. For the asymptotic values E_∞ of the calculated energies we get $1.009\,203$ MeV for even and $1.009\,198$ MeV for odd r.

For the distance $\bar{d} = 16$ we show some results of the minimisation process for the spin singlet configuration. In Fig. 8 we compare the $\vec{q}$-field in the initial and final configuration in a restricted region. The minimisation modifies especially the field in the region between the charges. The final
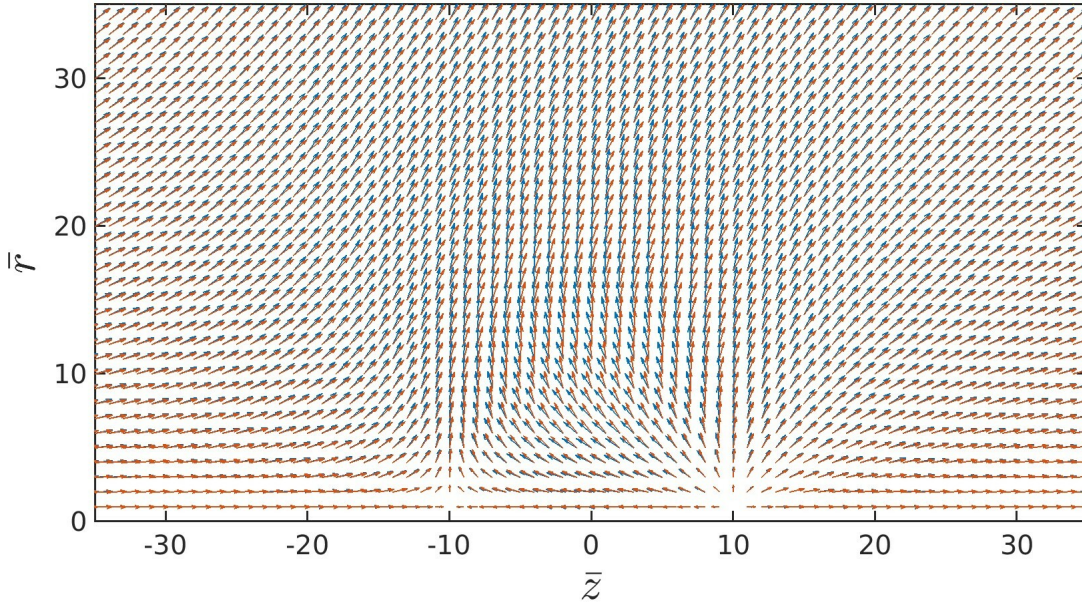

Figure 8: The modification of the imaginary part $\vec{q}(r,z)$ of the soliton field is represented by arrows. The initial configuration is shown in blue and the result of the minimisation process in red. Only a subregion of the 45×111-lattice is shown. Due to the finite size of solitons, $\bar{r}_0 = 3$, the centres of the charges the length of the arrows approaches zero as described by Eq. (2.6).

values of the real part q_0 of the soliton field are shown in Fig. 9. We observe that the distribution of q_0 values seems much broader than the distribution of the energy density in Fig. 10 with very

pronounced peaks reflecting the finite self energy $\mathcal{H}$ of charges according to Eq. (A.1).
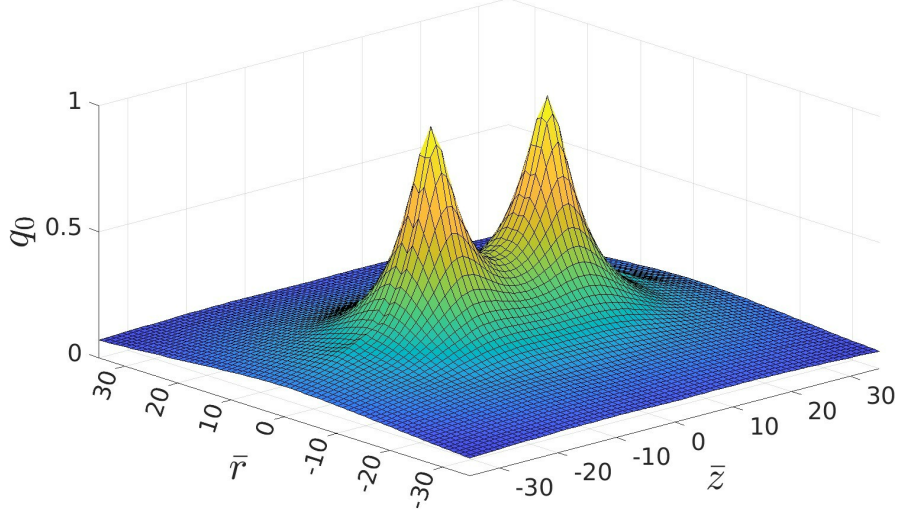

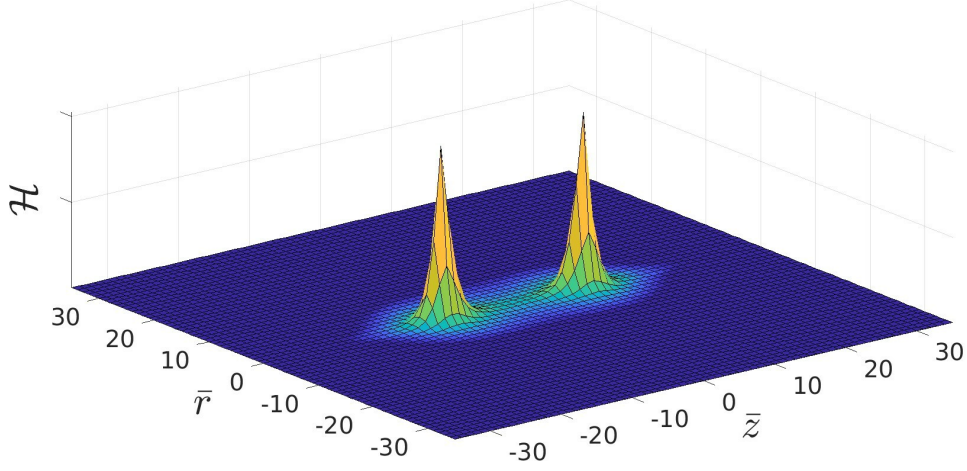Figure 9: q_0 distribution after minimisation for the configuration of Fig. 8.

Figure 10: Energy density after minimisation for the configuration of Fig. 8. Despite the regularisation of the self-energy of charges by the finite soliton size $\bar{r}_0 = 3$ there exist still very pronounced peaks of the energy density $\mathcal{H}$ according to Eq. (A.1) at the charge centres.

References

[1] Manfried Faber. A model for topological fermions. *Few Body Syst.*, 30:149–186, 2001.

[2] Manfried Faber. A geometric model in 3+1d space-time for electrodynamic phenomena. *Universe*, 8(2):73, 2022.

[3] Paul A. M. Dirac. Quantised singularities in the electromagnetic field. *Proc. Roy. Soc. Lond.*, A133:60–72, 1931.

[4] Paul A. M. Dirac. The theory of magnetic poles. *Phys. Rev.*, 74:817–830, 1948.

[5] R. A. Millikan. On the elementary electrical charge and the avogadro constant. *Phys. Rev.*, 2:109–143, Aug 1913.

[6] J.D. Jackson. *Classical electrodynamics*. Wiley, 1999.

[7] Tai Tsun Wu and Chen Ning Yang. Concept of nonintegrable phase factors and global formulation of gauge fields. *Phys. Rev. D*, 12:3845–3857, Dec 1975.

[8] Tai Tsun Wu and Chen-Ning Yang. Some solutions of the classical isotopic gauge field equations. In Hans Mark and Sidney Fernbach, editors, *Properties of Matter Under Unusual Conditions*, pages 349–354. John Wiley & Sons, Inc., New York, 1969.

[9] Tai Tsun Wu and Chen Ning Yang. Some remarks about unquantized non-abelian gauge fields. *Phys. Rev. D*, 12:3843–3844, Dec 1975.

[10] Howard Georgi and Sheldon L. Glashow. Unified weak and electromagnetic interactions without neutral currents. *Phys. Rev. Lett.*, 28:1494, 1972.

[11] Gerard 't Hooft. MAGNETIC MONOPOLES IN UNIFIED GAUGE THEORIES. *Nucl. Phys.*, B79:276–284, 1974.

[12] Alexander M. Polyakov. Particle spectrum in quantum field theory. *JETP Lett.*, 20:194–195, 1974.

[13] M. Remoissenet. *Waves called solitons : concepts and experiments / M. Remoissenet.* Springer-Verlag, Berlin ;, 1999.

[14] T. H. R. Skyrme. A Nonlinear theory of strong interactions. *Proc. Roy. Soc. Lond. A*, 247:260–278, 1958.

[15] T. H. R. Skyrme. A Nonlinear field theory. *Proc. Roy. Soc. Lond. A*, 260:127–138, 1961.

[16] T. H. R. Skyrme. A Unified Field Theory of Mesons and Baryons. *Nucl. Phys.*, 31:556–569, 1962.

[17] Vladimir G. Makhankov, Yurii P. Rybakov, and Sanyuk Valerii I. *The Skyrme model.* Springer Series in Nuclear and Particle Physics. Springer-Verlag Berlin Heidelberg, 1993.

[18] C. Adam and A. Wereszczynski. Topological energy bounds in generalized Skyrme models. *Phys. Rev. D*, 89(6):065010, 2014.

[19] Manfried Faber and Alexander P. Kobushkin. Electrodynamic limit in a model for charged solitons. *Phys.Rev.*, D69:116002, 2004.

[20] Dmitry Borisyuk, Manfried Faber, and Alexander Kobushkin. Electro-Magnetic Waves within a Model for Charged Solitons. *J. Phys.*, A40:525–531, 2007.

[21] Manfried Faber, Alexander Kobushkin, and Mario Pitschmann. Shape vibrations of topological fermions. *Adv. Stud. Theor. Phys.*, 2:11–22, 2008.

[22] Anmasser F. Theuerkauf D. and Faber M. About the solution of the numerical instability for topological solitons with long range interaction. *Few-Body Systems*, 62(84), 2021.

[23] M.E. Peskin. *An Introduction To Quantum Field Theory (1st ed.).* CRC Press, 1995.

[24] Manfried Faber. From soft dirac monopoles to the dirac equation. *Universe*, 8(8):387, jul 2022.

[25] Joachim Wabnig. *Interaction in the Model of Topological Fermions.* Diploma thesis, Physics, Technische Universität Wien, 2001.

[26] Dominik Theuerkauf. *Charged particles in the model of topological fermions.* Diploma thesis, Physics, Technische Universität Wien, 2016.

[27] Fabian Anmasser. *Running coupling constant in the model of topological fermions.* Diploma thesis, Physics, Technische Universität Wien, 2021.